Available online at www.sciencedirect.com

ScienceDirect

Materials Today: Proceedings 1 (2014) 70 – 81

materialstoday: PROCEEDINGS
www.materialstoday.com/proceedings

The 1st International Joint Mini-Symposium on Advanced Coatings between Indiana University-Purdue University Indianapolis and Changwon National University

Effect of microarc oxidation time on electrochemical behaviors of coated bio-compatible magnesium alloy

Jiayang Liu, Weijie Zhang, Hanying Zhang, Xinyao Hu, Jing Zhang*

Department of Mechanical Engineering, Indiana University –Purdue University Indianapolis, Indianapolis, IN, 46202, USA

Abstract

Magnesium alloys are newly promising biomaterials with potential application of human bone replacement. However, there is a drawback due to their high corrosion rates. In this study, AZ31 magnesium alloys were coated using microarc oxidation (MAO) process. Two oxidation durations, 1 minute and 5 minutes, were used. The samples were immersed in the simulated body fluid (SBF) for up to seven days. Then the electrochemical behaviors of the two samples were comparatively investigated. Potentiodynamic polarization and electrochemical impedance spectroscopy (EIS) experiments were used. The results show that the 5-minute MAO coated sample had a better corrosion resistance than the 1-minute MAO coated sample. The study shows processing parameters, e.g., oxidation time, can be used to design an optimized MAO-coated magnesium alloy with controlled corrosion rates.

Selection and Peer-review under responsibility of the Chairs of The 1st International Joint Mini-Symposium on Advanced Coatings between Indiana University-Purdue University Indianapolis and Changwon National University, Indianapolis.

Keywords: AZ31 magnesium alloy; microarc oxidation; corrosion; simulated body fluid; potentiodynamic polarization;electrochemical impedance spectroscopy.

*Corresponding author. Tel.:+1-317-278-7186; fax: +1-317-274-9744.
E-mail address: jz29@iupui.edu

Selection and Peer-review under responsibility of the Chairs of The 1st International Joint Mini-Symposium on Advanced Coatings between Indiana University-Purdue University Indianapolis and Changwon National University, Indianapolis.
doi:10.1016/j.matpr.2014.09.014

1. Introduction

Degradable implant materials are designed to dissolve in the human body after the implants finish their tasks so that the second surgical procedure is unnecessary [1-3]. Magnesium and its alloys are great degradable temporary implant biomaterial because they can be gradually corroded away and dissolved by the human body. This characteristic can reduce the risk of complications effectively, which commonly occur after a surgery, and also decrease the cost of healing process. Another advantage of magnesium and its alloys is that the mechanical properties such as density, compressive yield strength and elastic modulus are close to those of human natural bone [2].

However, one of the key problems of the magnesium and its alloys is the fast corrosion rate when the material is immersed in the conductive environment such as human blood [4]. Magnesium is a very reactive element and has a very high corrosion rate, which can affect the ideal healing pace and cause the damage of bone tissue. This constraint restricts the application of the magnesium alloys to be a practically suitable implant. Thus, a useful and effective protection, such as protective coatings, has been studied by many researchers, to enhance the corrosion resistance.

Several coating approaches have been studied nowadays, to improve the ability for resisting corrosion of magnesium alloys, such as polymer coating [5], anodic oxidation [6, 7], and chemical conversion coating [8], and plasma iodization [9]. Microarc oxidation technique (MAO) is one of the most popular approaches due to the remarkable ability of improvement on corrosion resistance by producing a dense, thick and hard oxide coating on magnesium alloys [10, 11].

Much research has been discussed to assume the corrosion properties of MAO coated AZ31 Mg alloys and other Mg alloys by immersing in SBF, as well as sodium chloride solutions. Wang *et al* tested the MAO-coated AZ31 Mg alloy immersed in an alkaline electrolyte [12]. The results showed that the coating was porous, composing of MgO and Mg_2SiO_4. Srinivansan *et al* studied the phosphate-based coated AM50 magnesium alloy in NaCl solution [13]. Zhang *et al* [14] studied residual stress in the MAO-coated AZ Mg alloy using X-ray diffraction method. The results showed that stresses in the coating affected the mechanical and electrochemical properties.

In this study, two different MAO processing time samples, 1 minute and 5 minutes, were produced. The electrolyte of coating was 30g/L Na_2SiO_3, which has not been reported. The corrosion behaviors of MAO coated AZ31 magnesium alloy in the simulated body fluid were investigated.

2. Experimental

2.1 Preparation for samples

The chemical composition of magnesium alloy AZ31 is as follows (in wt.%): 2.5-3.5 Al,0.7~1.3 Zn, 0.2 Mn, 0.05 Si, 0.01 Cu, 0.005 Ni, 0.005 Fe, and Mg balance [14]. Before producing the MAO coating, all magnesium alloy samples were polished on various grade SiC papers until 1200 grit one. Then an ultrasonic metal agent was used to degrease the impurities on the surfaces of polished samples for 2 minutes. The samples were rinsed in deionized water for 1 min and ethyl alcohol for 2 min. Finally, the samples were dried in flowing air. The electrolyte applied for this study contained 30g/L Na_2SiO_3 solution. In this study, different oxidation times on AZ31, 1 minute and 5 minutes MAO coated samples are presented (Table 1).

Table 1 MAO processing parameters of the two samples

sample	oxidation time (min)	applied voltage (V)	pulse frequency (Hz)	concentration of Na_2SiO_3 electrolyte (g/L)
1 min MAO processing time	1	350	500	30
5 min MAO processing time	5	350	500	30

To simulate the body environment as close as possible, a simulated body fluid (SBF, Table 2) was introduced in the current study to understand the corrosion behavior of coated samples [15-17]. The SBF was replenished every day.

Table 2 Reagents for preparation of SBF (pH 7.25, 1L) [15]

Reagent	Purity (%)	Amount
NaCl	99.5	7.996 g
$NaHCO_3$	99.5-100.5	0.350 g
KCl	99.0	0.224 g
$K_2HPO_4 \cdot 3H_2O$	99.0	0.228 g
$MgCl_2 \cdot 6H_2O$	99.0	0.305 g
1 kmol/m^3 HCl	-	40 ml
$CaCl_2$	96.0	0.278 g
Na_2SO_4	99.0	0.071 g
$(CH_2OH)_3CNH_2$	99.9	6.057 g
1kmol/m^3 HCl	-	Adjusting pH

2.2 Electrochemical tests

Potentiodynamic polarization test was used to measure Tafel curves, which provide information on the corrosion potential and corrosion rate. Electrochemical impedance spectroscopy (EIS), was also used to measure Nyquist curves, which characterize the interface electrochemical properties between the simulated body fluid and AZ31 magnesium alloy.

All electrochemical tests used a three-electrode procedure, which included a silver/silver chloride reference electrode (Accumet electrode 13-620-216, Fisher Scientific) and a platinum foil (Fisher Scientific) as the counter electrode. All testing data were collected using an electrochemical tester (Solartron Electrochemical interface SI1287 and Impedance/Gain-phase analyzer SI1260). The area of the working electrode (AZ 31 magnesium alloy sample) immersed in the solution was around 4 cm^2. All tests were executed at room temperature of 28±1.0 °C. All samples were wrapped by wax at the joint between the electrode clip and sample. The scanning rate of Tafel curves was 0.5 mV/s from -0.300 V to 0.300 V. The electrochemical impedance spectroscopy tests were surveyed in the range of 5 Hz to 150 kHz, and the voltage amplitude was 5mV. The equivalent circuit model (ECM) was built and the EIS data were fitted by using Zsimpwin software.

2.3 Sample microstructure observation

Before immersion tests in the simulated body fluid, the surface and cross-section of the magnesium ally samples were studied using a scanning electron microscopy. After specimens were removed from simulated body fluid, the microscopic surface morphologies of the samples were observed by an Amscope optical microscope immediately. In the same time, the macroscopic images of surface figure were also taken by a portable digital camera.

3. Results and discussion

3.1 Microstructure of specimen and porosity evaluation

Figure 1 shows the SEM image of the sample surfaces before immersion tests. Typical MAO porous microstructures were present on the coatings. For the 1-minute MAO processing coated sample, larger size pores were observed on the surface. For the 5-minute oxidation one, a large amount of micropores occurred on the coating surface. The pores served as the microarc discharging channels during the MAO process [14]. At the initial stage of oxidation, the undissolved solvent was accumulated near the substrate. With the increase of time, more liquid melt dissolved in the solution so that it covered those small micropores.

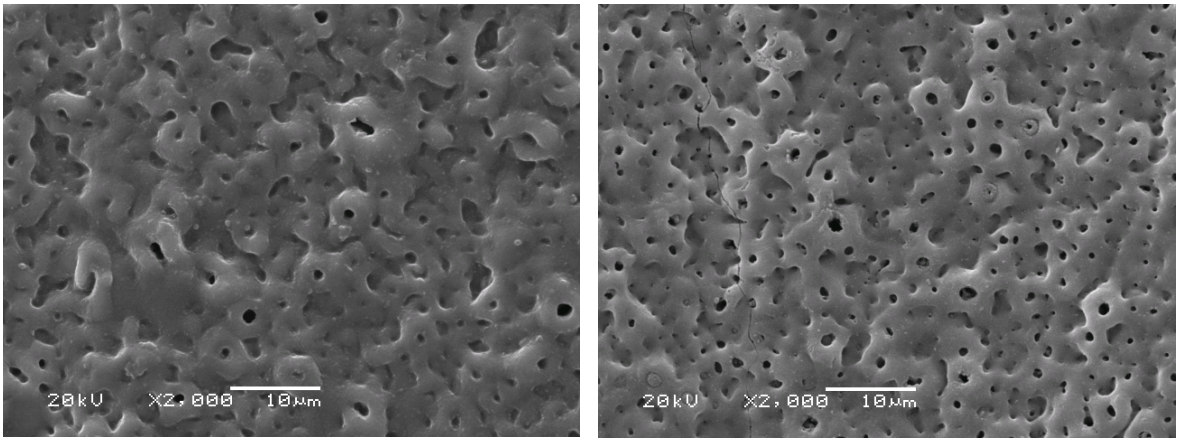

(a) (b)

Fig. 1. Surface morphologies of MAO coated samples produced at different oxidation durations (a) 1 minute; (b) 5 minutes.

The initial porosity of the MAO-coated magnesium alloys is a very important piece of information to estimate the corrosion resistance. The pores can affect the interaction between the SBF solution and the magnesium substrate after the solution penetrates through those pores. The porosity of the MAO-coated samples was evaluated according to the potentiodynamic polarization data after the samples being immersed in the SBF for a period of 0.5 hour. The porosity (F) is calculated by [18, 19]:

$$F = (\frac{R_{pm}}{R_p}) \times 10^{-|\Delta E_{corr}/\beta_{uncoated}|} \quad (1)$$

where, R_p (Ω*cm^2)and R_{pm} (Ω*cm^2) are the polarization resistance of the MAO-coated samples and uncoated samples, respectively. The ΔE_{corr} (V) is the difference of corrosion potential between the uncoated and coated samples, and $\beta_{uncoated}$ is the anodic Tafel constant of the uncoated sample. $\beta_{uncoated}$ of 92.2 mV/decade and Ecorr of uncoated samples of -1.4779 V were used in the calculation. R_{pm} equals 803 Ω*cm^2. The polarization resistance (R_p) is calculated by the Stern-Geary equation [20]:

$$R_p = \frac{\beta_a \beta_c}{2.3 I_{corr} (\beta_a + \beta_c)} \quad (2)$$

where, I_{corr} is the corrosion current density, β_c is the cathodic Tafel constant.

Table 3 shows the data using in Eq. (1) and Eq. (2), and the calculation results of porosity of MAO coated samples produced at different oxidation times. The porosity of MAO-coated samples decreased with increasing MAO processing time. Therefore, the 5 minutes MAO-coated samples can provide higher density.

Table 3 Tafel data for MAO-coated AZ31 Mg alloys and porosity after immersion in the SBF for 0.5h

sample	Ecorr (V)	Icorr (mA/cm^2)	βa (mv/decade)	βc (mv/decade)	Rp (Ω*cm^2)	porosity (%)
1 min MAO processing time	-1.4901	0.0031	102.21	208.32	9633	6.14
5 min MAO processing time	-1.4219	0.0051	75.25	245.25	5109	4.03

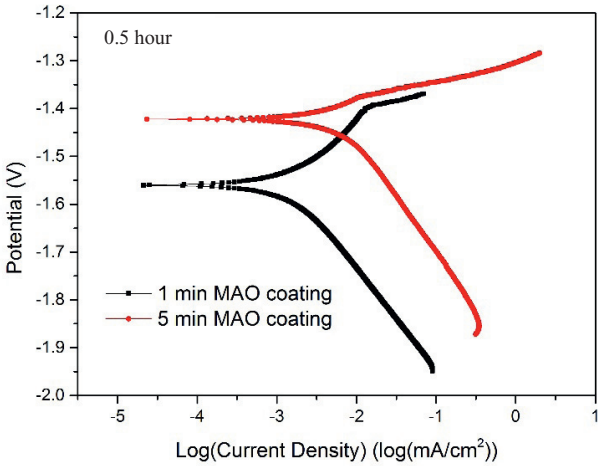

Fig 2. Tafel plot of MAO-coated AZ31 Mg alloy after immersion in the SBF for 0.5 hour

The Tafel curves for the MAO-coated AZ31 magnesium alloys after immersion in the SBF for 0.5 hour are illustrated in Figure 2. The cross-sectional views of the coatings are illustrated in Figure 3. It can be seen that the MAO coating thickness increased with increasing oxidation time. For the 1-minute MAO processing time sample, the thickness was 3.11±0.43μm. For the sample with 5-minutes MAO processing time, the thickness was 3.19±0.61 μm. More pores can be seen on 1 min MAO processing sample. This is due to less oxidation time. The smaller coating thickness is due to the shortest oxidation time. The sample coated for 5 min shows a thicker coating layer with a smoother and uniform microstructure with fewer micro pores, compared to the 1 minute oxidation time sample.

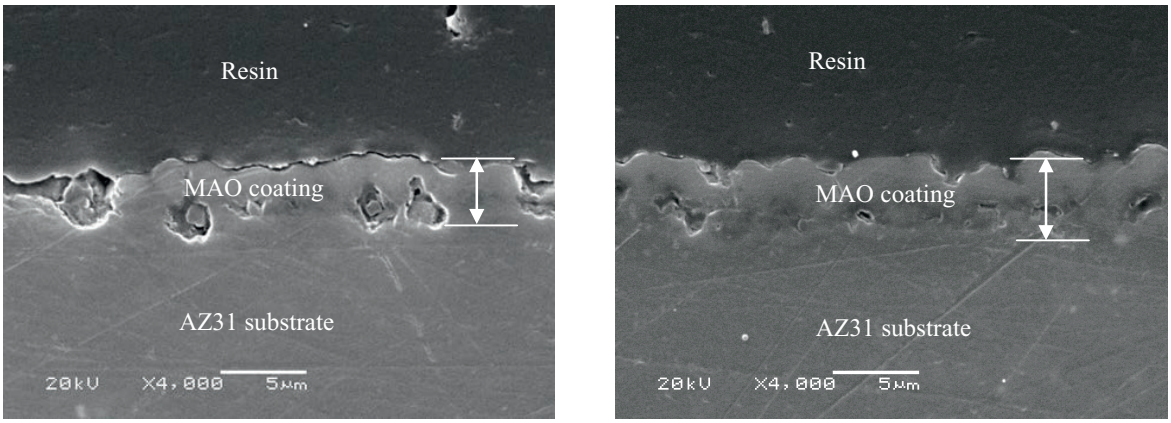

(a) (b)

Fig. 3. Cross-sectional views of MAO coated samples produced at different oxidation times (a) 1 minute; (b) 5 minutes

3.2 Potentiodynamic polarization tests

Figure 4 shows the polarization curves of the MAO coated samples produced at 1 minute and 5 minutes after 1 day, 3 days, 5 days and 7 days immersion in the simulated body fluid. From the Tafel curves, the corrosion potential (E_{corr}) and corrosion current density (I_{corr}) can be determined. The results are shown in Table 4.

Table 4 Corrosion potential (E_{corr}) of MAO-coated samples after 7 days immersion in the SBF

Samples	1 min MAO processing	5 min MAO processing
1 day immersion	-1.3070	-1.3203
3 day immersion	-1.3126	-1.3394
5 day immersion	-1.3512	-1.3445
7 day immersion	-1.3443	-1.3492

From Table 4, it can be found that the E_{corr} of both coated samples were decreased. Also, on the 1 day and 3 day, the E_{corr} of the 5-minute MAO coated specimen was lower than the 1-minute one. However after 7 days of immersion, and the E_{corr} of coated samples became similar. This is due to the fact that coating layers dissolved in the SBF after 7 days. The corrosion current density I_{corr} for the MAO coated samples are presented in Table 5.

Table 5 Corrosion current density (mA/cm^2) of MAO-coated samples after 7 days immersion in the SBF

Samples	1 min MAO processing	5 min MAO processing
1 day immersion	0.0208	0.03344
3 day immersion	0.0471	0.69183
5 day immersion	0.0841	0.07156
7 day immersion	0.0863	0.07446

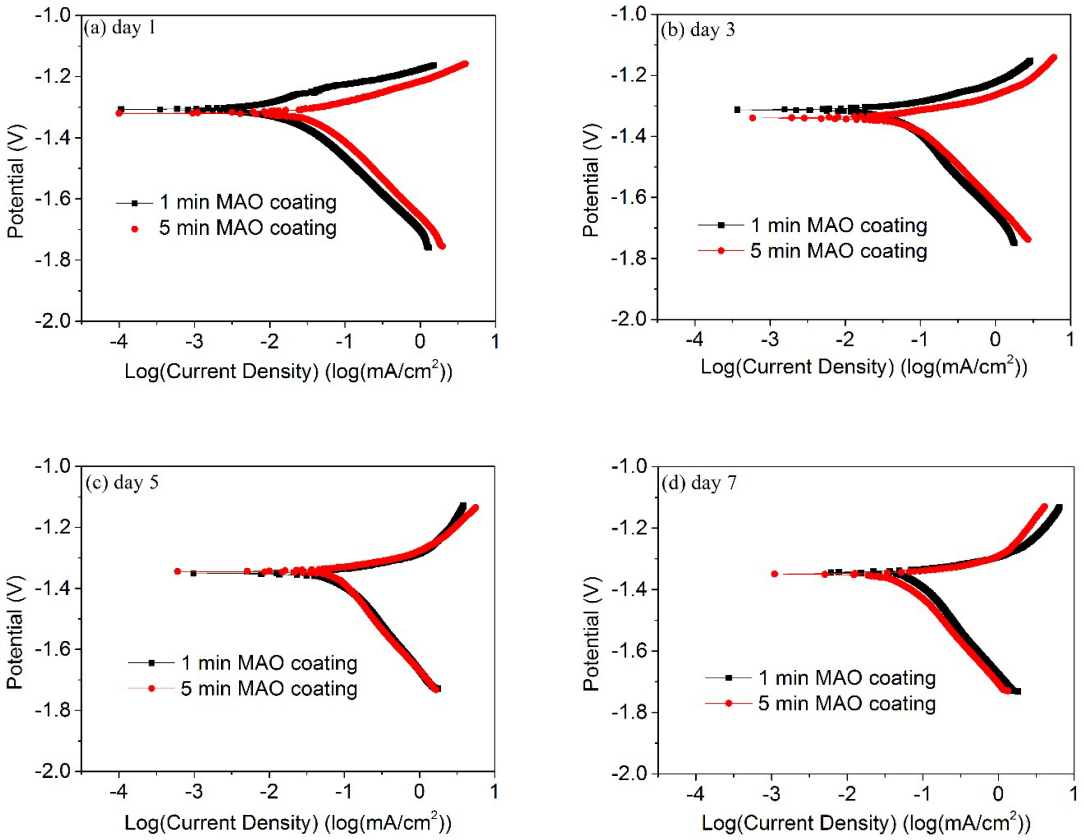

Fig. 4. Tafel plots of MAO-coated AZ31 Mg alloy after immersion in the SBF for (a) 1 day; (b) 3 days; (c) 5 days (d) 7 days

According to Table 5 and Tafel curves in Figure 4, it is clear that at the beginning of the corrosion occurred, both samples had a similar I_{corr}. The 5-minute MAO coated samples had the lower corrosion current density than the 1-minute one. This suggested that the 5-minute sample has the better corrosion resistance.

3.3 Electrochemical impedance spectroscopy tests

The Nyquist plots of the MAO-coated AZ31 alloys samples immersing in SBF for different durations are presented in Figure 5. It shows that the 5-minute sample had the higher impedance than the 1-minute sample. This result agreed with the Tafel data that the 5-minute sample has better corrosion resistance.

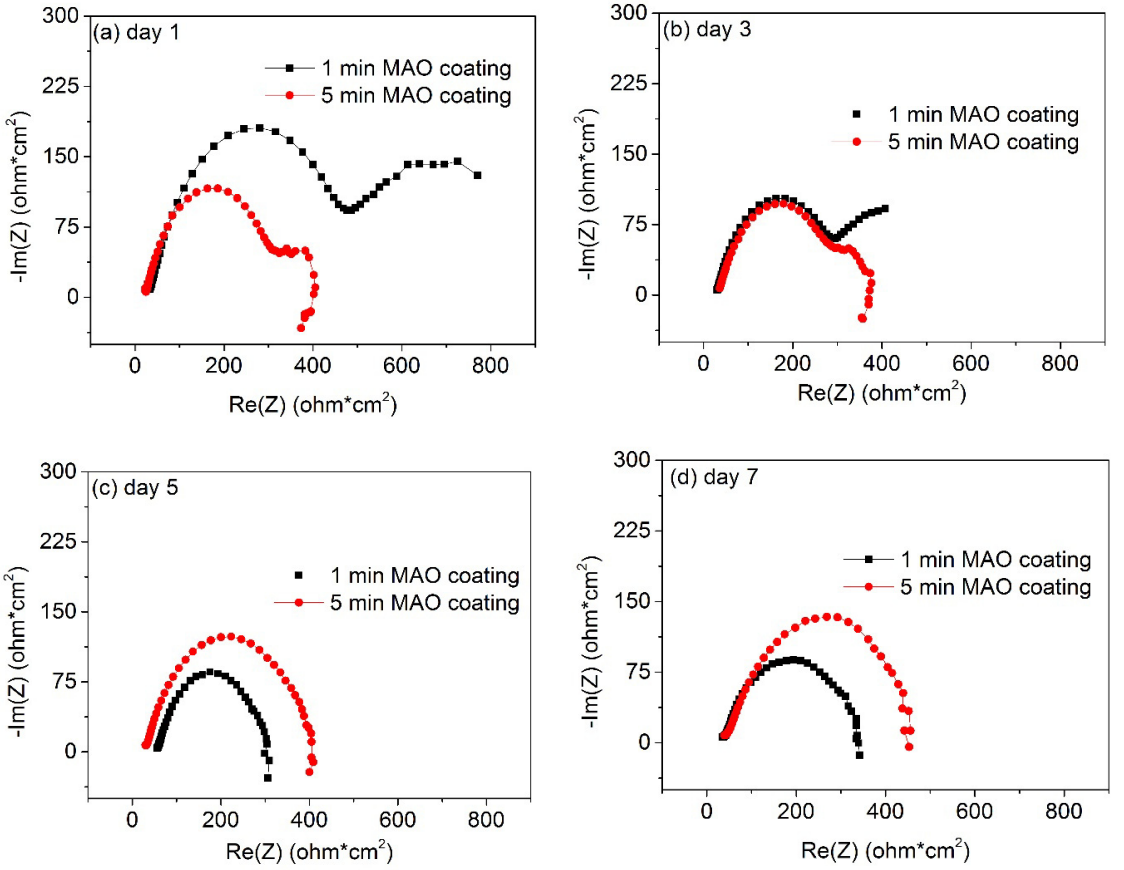

Fig. 5 Nyquist plots of MAO-coated AZ31 Mg alloy after immersion in the SBF for (a) 1 day; (b) 3 days; (c) 5 days; (d) 7 days

According to the Nyquist curves, an equivalent circuit model was built, as shown in Figure 6. There are two types of equivalent circuits to simulate the electrochemical behaviors [21-23]. Fig. 6 (a) was used to fit the Nyquist curves from the first day to the third day on the MAO-coated samples. After immersing in the SBF for 3 days, the MAO coatings dissolved into the solution and the substrate layers were exposed in the solution. This phenomenon was also shown in Figure 5 where two half circles were present in day 1 and day 3 (Fig. 5 a & b). While only one half circle in day 5 and day 7 (Fig. 5 c & d). When major coating parts dissolved away from the substrate, the coated samples behaved similar to the uncoated AZ31 magnesium alloy.

The charge transfer resistance, Rct, is a parameter characterizing the corrosion behavior of coated samples. The results of equivalent circuit are summarized in Table 6. The larger the Rct is, the lower corrosion rate the sample has [24]. From Table 6, in general, the 5 minutes MAO coated sample had a higher charge transfer resistance in day 1, day 5 and day 7. That means the 5 minutes MAO coated sample has better ability for corrosion resistance.

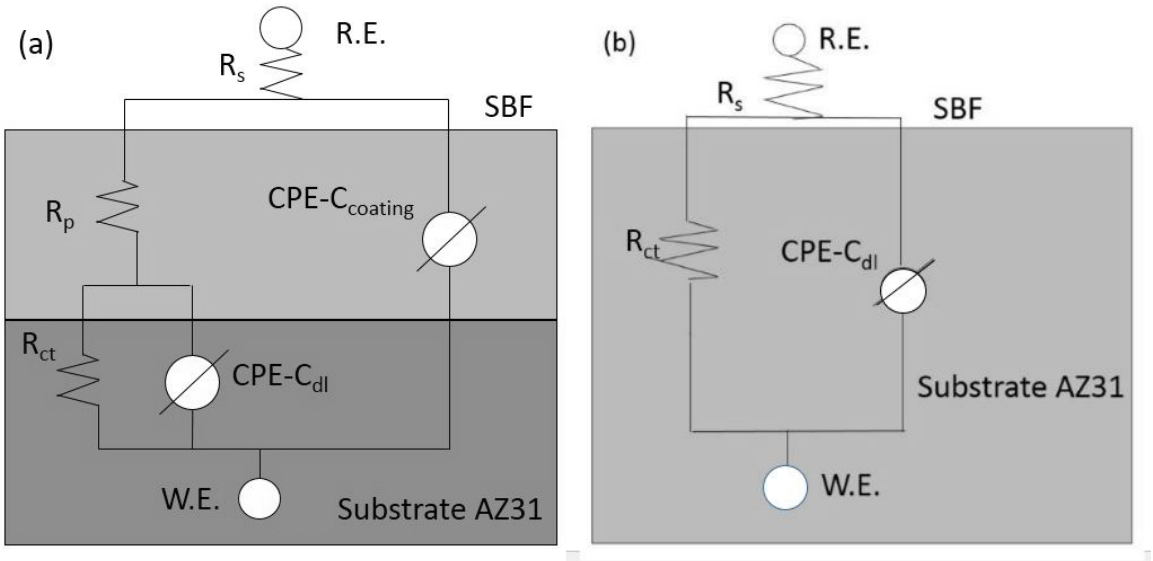

Fig. 6. Equivalent circuits for fitting the electrochemical corrosion behaviors. Rs represents the solution resistance between the reference electrode and working electrode, Rct is the resistance of charge transfer between the MAO coating and substrate. Cdl, which is in parallel with Rct, is the CPE of the double layer. R_p is the resistance of the MAO coating from the porous regions, paralleling with CPE-$C_{coating}$. (a) MAO-coated samples from day 1 to day 3; (b) MAO coated samples from day 4 to day 7

Table 6 Equivalent circuit model data

sample	immersion time (day)	Rs (Ωcm^2)	CPE-Ccoating (μF)	Rp(Ωcm^2)	CPE-Cdl(μF)	Rct(Ωcm^2)
1 min MAO processing time	1	31.46	35.86	497.3	2126	283.3
	3	29.64	53.81	288.6	2415	175.7
	5	56.58	-	-	78.45	251.8
	7	38.32	-	-	81.72	320
5 min MAO processing time	1	21.16	39.99	371.3	2707	347
	3	33.66	82.17	282.1	4272	56.7
	5	29.8	-	-	64.49	382.6
	7	40.49	-	-	87.27	477

3.4 Surface microscopic and macroscopic images after immersion

The surface microscopic and macroscopic morphologies of MAO coated samples during the 7 days immersion time are shown in Figure 7 and Figure 8, respectively. According to the microscopic images (Fig. 7), the evaluations of the corrosion damage were observed. It shows that the surfaces of MAO coated samples had been protected by dense coating layer in the beginning days of immersion. While the dark areas increased with the increasing time. At the end of seven days of immersion, the coatings were totally dissolved in the solution. The formation and promotion of pits were caused by prior large cathodic polarization [25].

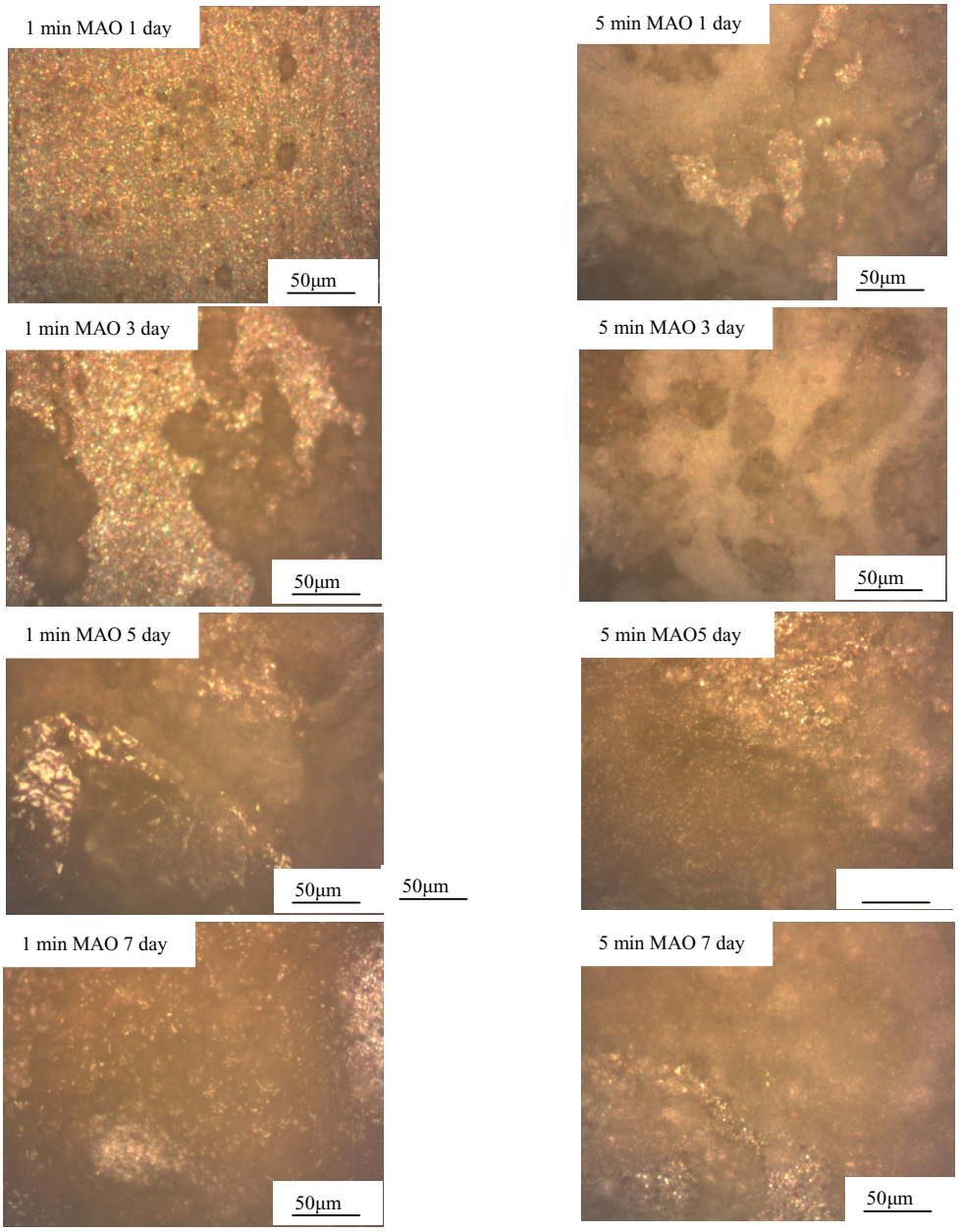

Fig. 7. Surface microscopic images of MAO coated AZ31 magnesium alloy after immersion in the SBF for various duration

The similar results can be obtained from the macroscopic images as shown in Fig. 8. It is clearly that the size of the samples decreased with the immersion time. The 1-minute MAO coated sample had the higher corrosion rate due to the largest loss of sample size, which is in agreement with the electrochemical test results. Furthermore, the 5-minute MAO coated sample almost kept the original size. In other words, the 5-minute MAO coating can provide an effective protection for the AZ31 magnesium alloys.

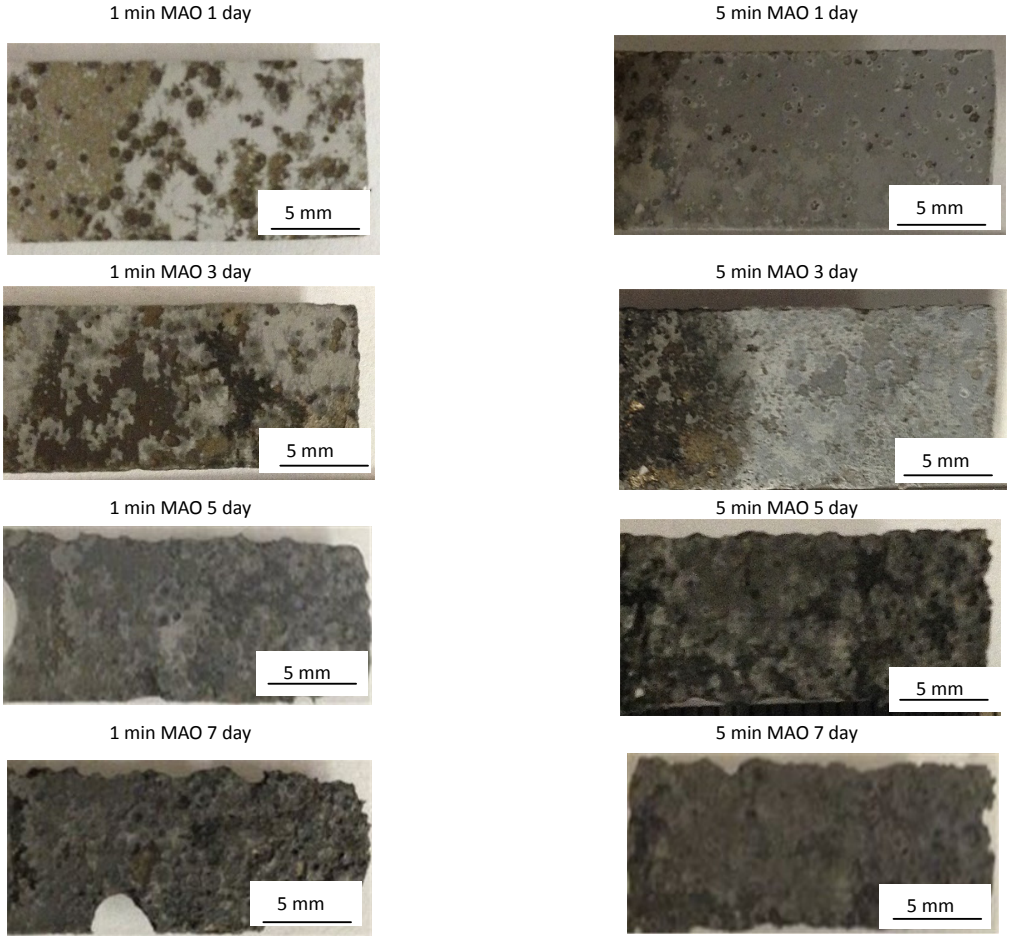

Fig. 8. Surface microscopic images of the MAO coated AZ31 magnesium alloy after immersion in the SBF for various durations

4. Conclusions

Two MAO coated samples with different processing oxidation times, 1 minute and 5 minutes were tested in this study. The corrosion behaviors of the two coated samples were comparative studied. The following conclusions have been determined.

(1) The results of potentiodynamic polarization and electrochemical impedance spectroscopy indicated that the 5-minute MAO sample possessed the best corrosion resistance between the two tested samples. The result was also confirmed by the surface micrographs and macrographs after 7 days immersion in the simulated body fluid.

(2) The equivalent circuit models were developed in this study to investigate the corrosion mechanism of MAO coated AZ31 magnesium alloys. It shows that the 5-minute MAO coated sample produced by Na_2SiO_3 can provide a better charge transfer resistance than 1 minute one after 7 days immersion.

Acknowledgement

The authors acknowledge the financial support provided by the IUPUI International Development Fund and IUPUI Multidisciplinary Undergraduate Research Institute (MURI). Thanks for the MAO samples provided by Professor Chengyun Ning at South China University of Technology, the EIS experiment assistance by Professor Jian Xie and Dr. Yadong Liu, and SEM images by Prof. Yeon-Gil Jung at Changwon National University.

References

1. Zhang, R.F., G.Y. Xiong, and C.Y. Hu, *Comparison of coating properties obtained by MAO on magnesium alloys in silicate and phytic acid electrolytes.* Current Applied Physics, 2010. **10**(1): p. 255-259.
2. Staiger, M.P., et al., *Magnesium and its alloys as orthopedic biomaterials: A review.* Biomaterials, 2006. **27**(9): p. 1728-1734.
3. Dai, Y., et al., *Effects of five additives on electrochemical corrosion behaviours of AZ91D magnesium alloy in sodium chloride solution.* Surface Engineering, 2011. **27**(7): p. 536-543.
4. Kirkland, N.T., et al., *A survey of bio-corrosion rates of magnesium alloys.* Corrosion Science, 2010. **52**(2): p. 287-291.
5. Wong, H.M., et al., *A biodegradable polymer-based coating to control the performance of magnesium alloy orthopaedic implants.* Biomaterials, 2010. **31**(8): p. 2084-2096.
6. Gonzalez-Nunez, M.A., et al., *A non-chromate conversion coating for magnesium alloys and magnesium-based metal matrix composites.* Corrosion Science, 1995. **37**(11): p. 1763-1772.
7. Mizutani, Y., et al., *Anodizing of Mg alloys in alkaline solutions.* Surface and Coatings Technology, 2003. **169–170**(0): p. 143-146.
8. Yue, T.M., A.H. Wang, and H.C. Man, *Improvement in the corrosion resistance of magnesium ZK60SiC composite by excimer laser surface treatment.* Scripta Materialia, 1997. **38**(2): p. 191-198.
9. Hoche, H., et al., *Plasma anodisation as an environmental harmless method for the corrosion protection of magnesium alloys.* Surface and Coatings Technology, 2003. **174–175**(0): p. 1002-1007.
10. Lee, Y.K., K. Lee, and T. Jung, *Study on microarc oxidation of AZ31B magnesium alloy in alkaline metal silicate solution.* Electrochemistry Communications, 2008. **10**(11): p. 1716-1719.
11. Yerokhin, A.L., et al., *Plasma electrolysis for surface engineering.* Surface and Coatings Technology, 1999. **122**(2–3): p. 73-93.
12. Wang, H.M., Z.H. Chen, and L.L. Li, *Corrosion resistance and microstructure characteristics of plasma electrolytic oxidation coatings formed on AZ31 magnesium alloy.* Surface Engineering, 2010. **26**(5): p. 385-391.
13. Bala Srinivasan, P., et al., *Effect of pulse frequency on the microstructure, phase composition and corrosion performance of a phosphate-based plasma electrolytic oxidation coated AM50 magnesium alloy.* Applied Surface Science, 2010. **256**(12): p. 3928-3935.
14. Zhang, J., et al., *Electrochemical behavior of biocompatible AZ31 magnesium alloy in simulated body fluid.* Journal of Materials Science, 2012. **47**(13): p. 5197-5204.
15. Kokubo, T. and H. Takadama, *How useful is SBF in predicting in vivo bone bioactivity?* Biomaterials, 2006. **27**(15): p. 2907-2915.
16. Song, Y.W., et al., *Biodegradable behaviors of AZ31 magnesium alloy in simulated body fluid.* Materials Science & Engineering C-Biomimetic and Supramolecular Systems, 2009. **29**(3): p. 1039-1045.
17. Wang, Y., et al., *Corrosion process of pure magnesium in simulated body fluid.* Materials Letters, 2008. **62**(14): p. 2181-2184.
18. Laleh, M., et al., *Effect of alumina sol addition to micro-arc oxidation electrolyte on the properties of MAO coatings formed on magnesium alloy AZ91D.* Journal of Alloys and Compounds, 2010. **496**(1–2): p. 548-552.
19. Liu, C., et al., *An electrochemical impedance spectroscopy study of the corrosion behaviour of PVD coated steels in 0.5 N NaCl aqueous solution: Part II.: EIS interpretation of corrosion behaviour.* Corrosion Science, 2003. **45**(6): p. 1257-1273.
20. Jones, D.A., *Principles and prevention of corrosion*1996: Prentice Hall.

21. Ahn, S.H., et al., *A study on the quantitative determination of through-coating porosity in PVD-grown coatings.* Applied Surface Science, 2004. **233**(1–4): p. 105-114.
22. Ghasemi, A., et al., *Study of the structure and corrosion behavior of PEO coatings on AM50 magnesium alloy by electrochemical impedance spectroscopy.* Surface and Coatings Technology, 2008. **202**(15): p. 3513-3518.
23. Liang, J., et al., *Electrochemical corrosion behaviour of plasma electrolytic oxidation coatings on AM50 magnesium alloy formed in silicate and phosphate based electrolytes.* Electrochimica Acta, 2009. **54**(14): p. 3842-3850.
24. Xu, R., et al., *Improved corrosion resistance on biodegradable magnesium by zinc and aluminum ion implantation.* Applied Surface Science, 2012. **263**(0): p. 608-612.
25. Lee, W.-J. and S.-I. Pyun, *Role of prior cathodic polarization in the pitting corrosion of pure aluminium in acidic chloride solution.* Materials Science and Engineering: A, 2000. **279**(1–2): p. 130-137.